doi:10.1016/j.jmb.2005.04.044 J. Mol. Biol. (2005) 350, 395–401

JMB

Available online at www.sciencedirect.com

SCIENCE DIRECT®

ELSEVIER

COMMUNICATION

Hydroxyl Groups in the ββ Sandwich of Metallo-β-lactamases Favor Enzyme Activity: A Computational Protein Design Study

Peter Oelschlaeger[1] and Stephen L. Mayo[2]*

[1]*Division of Biology, California Institute of Technology, Mail Code 114-96, Pasadena, CA 91125, USA*

[2]*Howard Hughes Medical Institute, Divisions of Biology and Chemistry and Chemical Engineering, California Institute of Technology, Mail Code 114-96, Pasadena, CA 91125, USA*

**Corresponding author*

Metallo-β-lactamases challenge antimicrobial therapies by their ability to hydrolyze and inactivate a broad spectrum of β-lactam antibiotics. The potential of these enzymes to acquire enhanced catalytic efficiency through mutation is of great concern. Here, we explore the potential of computational protein design to predict mutants of the imipenemase IMP-1 that modulate the catalytic efficiency of the enzyme against a range of substrates. Focusing on the four amino acid positions 69, 121, 218, and 262, we carried out a number of design calculations. Two mutant enzymes were predicted: the single mutant S262A and the double mutant F218Y-S262A. Compared to IMP-1, the single mutant (S262A) results in the loss of a hydroxyl group and the double mutant (F218Y-S262A) results in a hydroxyl transfer from position 262 to position 218. The presence of both hydroxyl groups at positions 218 and 262 was tested by examining the mutant F218Y. Kinetic constants of IMP-1, the two computationally designed mutants (S262A and F218Y-S262A), and the hydroxyl addition mutant (F218Y) were determined with seven substrates. Catalytic efficiencies are highest for the enzyme with both hydroxyl groups (F218Y) and lowest for the enzyme lacking both hydroxyl groups (S262A). The catalytic efficiencies of the two enzymes with one hydroxyl group each are intermediate, with the F218Y-S262A double mutant exhibiting enhanced hydrolysis of nitrocefin, cephalothin, and cefotaxime relative to IMP-1.

Keywords: metallo-β-lactamase; zinc β-lactamase; protein design; catalytic efficiency; substrate specificity

Metallo-β-lactamases (MBLs) are important components of the bacterial defense mechanism against antibiotics. They catalyze the hydrolysis and inactivation of β-lactam substrates such as penicillins, cephalosporins, and carbapenems. Over the last decade, they have become a worldwide clinical problem due to their broad substrate spectra, potential for horizontal transference, and the absence of clinically useful inhibitors. All MBLs exhibit a unique αββα fold; the active site consists of two zinc-binding sites and is located at one edge of the ββ sandwich.[1] The Zn1 binding site is formed by His, Asn, or Gln at position 116, and His at positions 118 and 196, while Zn2 is ligated by Asp120, Cys221, and His263.[2] Most MBLs show maximum activity only when two zinc ions are bound, and the employment of Zn2 has been interpreted as an evolutionary adaptation to improve catalytic efficiency.[3] An important function of Zn2 is to stabilize an anionic intermediate, in which the amide bond of the β-lactam ring is cleaved, but the emerging nitrogen atom is not protonated.[4,5] The anionic intermediate is coordinated to Zn1 *via* the carboxyl group and to Zn2 *via*

Present address: P. Oelschlaeger, Warshel Group, Department of Chemistry, SGM 418, University of Southern California, 3620 McClintock Ave., Los Angeles, CA 90089, USA.

Abbreviations used: MBL, metallo-β-lactamase; IMP, imipenem; MD, molecular dynamics; CAZ, ceftazidime; LOR, cephaloridine; PEN, benzylpenicillin; AMP, ampicillin; CEF, cephalothin; CTX, cefotaxime; NIT, nitrocefin.

E-mail address of the corresponding author: steve@mayo.caltech.edu

the anionic nitrogen atom resulting from amide bond cleavage.[5] The enhanced stability of the enzyme-substrate intermediate complex results in significantly increased k_{cat} and k_{cat}/K_M values for the binuclear MBL CcrA from *Bacteroides fragilis* compared to the corresponding mononuclear enzyme,[3] and the breakdown of the intermediate becomes the rate-limiting step.[3–5] Binuclear MBLs can improve catalytic efficiency further by mutating residues other than the essential zinc ligands. This is well documented for the imipenemases (IMP-*n*). IMP-1 likely evolved from IMP-3[6] *via* IMP-6;[7] IMP-1 differs from IMP-6 and IMP-3 by only one and two mutations, respectively. Molecular dynamics (MD) simulations indicate that Ser262 in IMP-1 supports the zinc ligand His263 in the presence of certain substrates (ceftazidime, CAZ; cephaloridine, LOR; benzylpenicillin, PEN; ampicillin, AMP; and imipenem, IMP) and leads to increased catalytic efficiencies compared to IMP-3 and IMP-6, which have Gly at position 262.[8] In contrast, other substrates (cephalothin, CEF; cefotaxime, CTX; and nitrocefin, NIT) are not affected significantly by the G262S mutation.[6,9] Materon and co-workers employed codon randomization to explore the effect of mutations in and near the active site of IMP-1 on antibiotic resistance.[10,11] They observed that cells harboring the S262G mutant were viable in the presence of CTX, but not in the presence of IMP, LOR, or AMP; in general, the sequence requirements for efficient inactivation of IMP, LOR, and AMP were found to be stricter than for inactivation of CTX.[11] In a study combining MD simulations to screen for novel MBL mutants and experimental determination of catalytic efficiencies, we observed that IMP-6 can easily improve hydrolysis of NIT, CEF, and CTX by point mutations, whereas only two of the point mutants investigated, G262A and G262S (IMP-1), exhibit improved conversion of CAZ, PEN, AMP, and IMP, with IMP-1 being the most efficient enzyme. On the basis of the different behavior of the tested substrates, we classified them as either type I (NIT, CEF, and CTX) or type II (LOR, CAZ, PEN, AMP, and IMP).[9] Type I substrates are converted well and many mutations improve conversion compared to IMP-1 and IMP-6; type II substrates are converted less efficiently and most mutations decrease catalytic efficiency relative to IMP-1.

Here, we explore the ability of computational protein design to predict efficient MBL mutants. In accordance with our previous study,[9] we designed positions 69, 121, 218, and 262 of IMP-1 (Figure 1). These residues are not directly in the active site, are not in contact with the substrate, and do not coordinate zinc. The coordinates of IMP-1 in complex with a mercaptocarboxylate inhibitor (chain A of PDB entry 1DD6)[12] were used as the template for computational design. Only single nucleotide changes in the IMP-6 gene that do not result in amino acids with altered charge or cysteine were allowed. Thus, the following amino acids were considered: Lys and Arg at position 69; Ser, Asn, Thr, Ile, and Gly at position 121; Phe, Leu, Ser, Tyr, Ile, and Val at position 218; and Gly, Ser, Ala, and Val at position 262. Possible side-chain conformations were represented by a backbone-dependent rotamer library[13] expanded by one standard deviation about $\chi1$ and $\chi2$ for all amino acids except Arg and Lys. The energy function used is based on the DREIDING force field[14] and includes a scaled van der Waals term,[15] hydrogen bonding and electrostatics terms,[16] and a surface area-based solvation term.[17] Since none of the designed residues is in contact with the zinc ions or the inhibitor, these were deleted prior to the calculations. In order not to disturb the zinc and inhibitor-depleted active site, zinc-ligating residues were fixed in their crystallographic conformations (Figure 1). In a first set of calculations (1A–C), all other residues of the protein except the designed

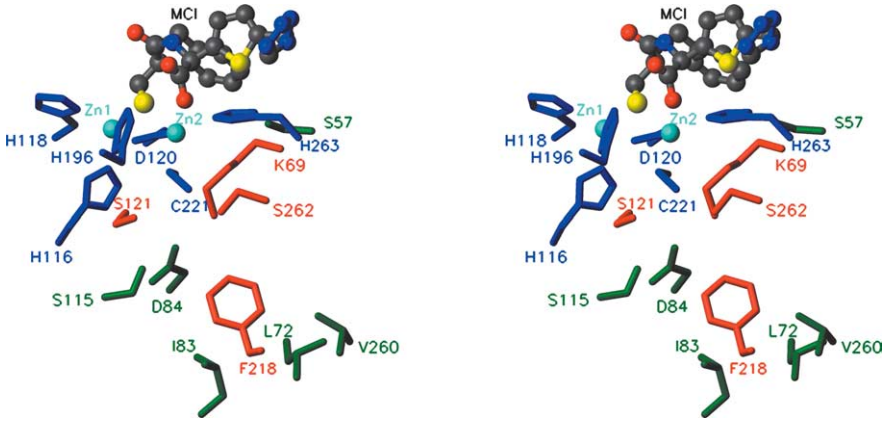

Figure 1. Stereo image of the IMP-1 active site and the designed residues. Although not included in the design, the mercaptocarboxylate inhibitor (MCI, balls and sticks, colored by atom: grey, C; red, O; blue, N; yellow, S) and the zinc ions (cyan spheres) are shown for orientation. The zinc ligands are shown in blue and were kept fixed in the design calculations. The redesigned residues are shown in orange. The residues floated in calculations 2A–C are shown in green. Molecular graphics were generated with MOLMOL.[28]

positions were fixed as well. In a second set of calculations (2A–C), all residues within a radius of 4 Å from the side-chain heavy atoms of the designed residues were floated; that is, allowed to change to a different rotamer while keeping the same amino acid identity (Figure 1). This was done to check whether movements of neighboring residues would change the design results. The floated residues were Ser57, Leu72, Ile83, Asp84, Ser115, and Val260. Each set of calculations consisted of three runs with different parameters. In 1A and 2A, a van der Waals scale factor, α, of 0.9 was used, in 1B, 1C, 2B, and 2C, α was set to 0.8; α determines the importance of packing in design calculations. Whereas 0.9 is the value of α used typically,[15] lower values can help compensate for the restrictive effects of a fixed backbone.[18] In calculations 1A, 1B, 2A, and 2B, the non-polar burial energy, σ_{np}, and the polar burial energy, σ_p, were 0.02 kcal mol^{-1} Å^{-2} and 0.04 kcal mol^{-1} Å^{-2}, respectively. In 1C and 2C, σ_{np} and σ_p were set to 0.026 kcal mol^{-1} Å^{-2} and 0.1 kcal mol^{-1} Å^{-2}, respectively (Table 1). An algorithm based on the dead-end elimination theorem[19,20] was used to obtain the minimum energy amino acid sequences and conformations.

Design calculations 1A, 1C, 2A, and 2C resulted in a point mutant, S262A. The identical enzyme, resulting from a G262A mutation in IMP-6, was predicted to exhibit high catalytic efficiencies in MD simulations (unpublished results). Experimental studies showed that the catalytic efficiencies of the G262A mutant of IMP-6 toward type I substrates equaled those of IMP-1 and IMP-6, whereas its efficiencies toward type II substrates were lower than those of IMP-1 but higher than those of IMP-6.[9] Due to the stringent van der Waals scale factor (α 0.9) in calculations 1A and 2A, and the high polar burial penalty (σ_p = 0.1 kcal mol^{-1} Å^{-2}) in calculations 1C and 2C, Ala was preferred over Ser. Interestingly, using a smaller van der Waals scale factor (α 0.8) in combination with a lower polar burial penalty (σ_p = 0.04 kcal mol^{-1} Å^{-2}) (calculations 1B and 2B) still did not produce wild-type Ser at this position, as might have been expected. However, in addition to the S262A mutation, the Phe at position 218 was replaced by Tyr. This F218Y-S262A double mutant of IMP-1 provides an interesting case study for a hydroxyl exchange from residue 262 to residue 218. In the designed proteins, the Tyr218 hydroxyl oxygen atom is 3.5 Å away from the position of the Ser262 hydroxyl oxygen atom in IMP-1. We have recently observed that Ser262 yields the highest catalytic efficiencies toward type II substrates[9] by supporting His263 through a domino effect:[8] the Ser side-chain fills in a hole next to His263 and interacts with Lys69; Lys69 for its part additionally stabilizes His263 *via* its neighbor Pro68, whose backbone hydrogen bonds to the His263 side-chain. The domino effect stabilizes the enzyme-substrate intermediate complex when the R_2 side-chain at C3 of cephalosporins or C2 of carbapenems is positively charged, or C2 of penicillins has axial methyl groups.[8] Here, we investigated whether the hydroxyl group on Tyr218 close to residue 262 has an effect similar to that of the hydroxyl group of Ser262. Another interesting aspect is that in the crystal structure of IMP-1 (PDB entry 1DD6)[12] the hydroxyl oxygen atom of Ser262, which is located in a loop of the C-terminal β-sheet, is very close (3.6 Å) to the side-chain nitrogen atom of Lys69, which is located in the opposite N-terminal β-sheet (Figure 2). Although not within hydrogen bonding distance in the crystal structure, an electrostatic interaction between these two residues might stabilize the ββ sandwich and facilitate protein folding. Also, Lys69 is located in one of the two antiparallel strands that extend into the β-hairpin loop covering the active site (residues 60–66). It has been shown that this loop, which includes Trp64, plays an important role in substrate binding and catalysis.[21,22] Thus, the interaction between Ser262 and Lys69 might be important for the proper orientation of this loop over the active site, effective substrate binding, and efficient catalysis. In the designed F218Y-S262A double mutant, the Tyr218 hydroxyl group is positioned to interact with Lys69: the distance between the Lys69 side-chain nitrogen atom and the Tyr218 hydroxyl oxygen atom is 2.8 Å. Thus, Tyr218 could play a role similar to Ser262, stabilizing the structure and facilitating catalytic activity.

The biophysical properties and catalytic efficiencies of the designed F218Y-S262A double mutant (henceforth named *OH-X* for hydroxyl exchange) were investigated experimentally and compared to those of IMP-1. We also studied two IMP-1 point mutants as controls: S262A, which has no hydroxyl groups on position 218 or 262 (named *OH-0*), and F218Y, which has hydroxyl groups on both residues (named *OH-2*). Models of all four enzymes are shown in Figure 2.

Using PCR-based site-directed mutagenesis, the

Table 1. Computational parameters and mutations resulting from the design calculations

Calculation	α	σ_{np} (kcal mol^{-1} Å^{-2})	σ_p (kcal mol^{-1} Å^{-2})	Mutations
1A	0.9	0.02	0.04	S262A
1B	0.8	0.02	0.04	F218Y, S262A
1C	0.8	0.026	0.1	S262A
2A	0.9	0.02	0.04	S262A
2B	0.8	0.02	0.04	F218Y, S262A
2C	0.8	0.026	0.1	S262A

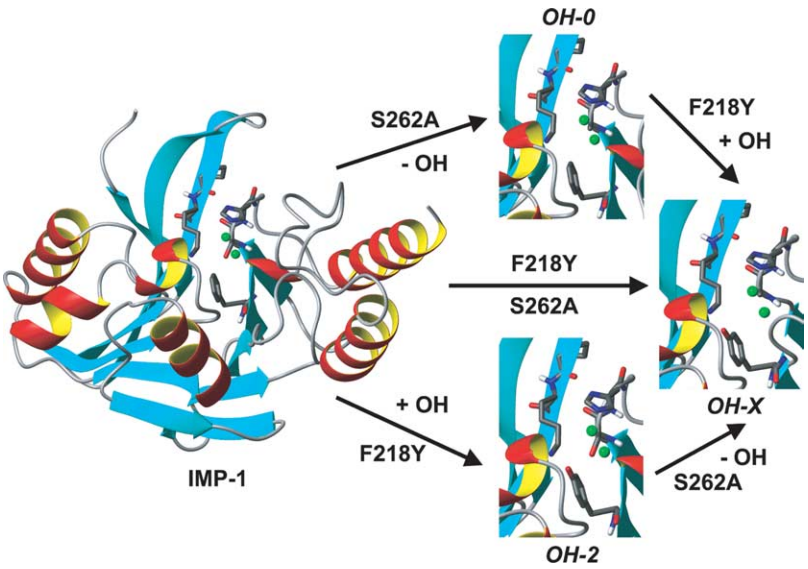

Figure 2. Model of IMP-1 structure (left) and the regions comprising residues 69, 218, and 262 of the mutant enzymes. The α-helices are shown as red and yellow ribbons, β-sheets are shown as cyan ribbons, and unordered loops are shown as grey tubes. Zinc ions are shown as green spheres. Lys69, Phe/Tyr218, Ser/Ala262, and the zinc ligand His263 are shown as sticks, colored by atom. Mutations and the net changes in the number of hydroxyl groups that led to each enzyme starting from IMP-1 are indicated with arrows.

desired mutations were introduced into the IMP-1 gene on a vector for cytoplasmic expression (kindly provided by Merck). All four enzymes were overexpressed successfully in *Escherichia coli* BL21(DE3) cells (Stratagene) with 20–60% found in the soluble fraction after cell lysis. All were purified and characterized as described.[9] The molecular masses determined by electrospray mass spectrometry corresponded to the theoretical values, and the zinc contents were between 1.6 and 2.0 zinc ions per molecule. In order to explore the impact of the hydroxyl groups at positions 218 and 262 on protein secondary structure and stability, we carried out circular dichroism (CD) wavelength scans and temperature melts (Figure 3). The CD wavelength scans produced for each of the purified enzymes were nearly superimposable (Figure 3(a)). The small differences in molar ellipticities are within the experimental error of the determination of protein concentration. For IMP-1 and *OH-2*, temperature melts yielded curves that could be fit to a two-state model (Figure 3(b)). The apparent (non-reversible) melting temperatures were 72 °C for IMP-1 and 71 °C for *OH-2*. In contrast, the melting curves obtained with *OH-0* and *OH-X* could not be fit to a two-state model. Up to 69 °C, the melting curve of *OH-X* was congruent with that of *OH-2*; however, unfolding was not complete until 82 °C compared to 78 °C for IMP-1 and *OH-2*. The unfolding curve of *OH-0* also exhibits non-two-state behavior. For *OH-X* and *OH-0*, the apparent melting temperatures were estimated to be 74 °C and 68 °C, respectively. Once unfolding was complete, no refolding was observed for any of the enzymes upon lowering the temperature, consistent with the proposal that zinc chaperones might be involved in zinc incorporation[23] and proper folding of MBLs.[24] Nevertheless, under physiological conditions all investigated enzymes are stable.

Kinetic constants of the four enzymes were determined with seven substrates; the catalytic efficiencies are shown in Figure 4 (and Table S1 in the Supplementary Data). Clearly, *OH-2* is the most efficient enzyme, exhibiting higher catalytic efficiencies toward all substrates except CTX, for which it equals *OH-X*. In contrast, *OH-0* is the least efficient enzyme. This observation suggests that hydroxyl groups at the ββ sandwich interface are beneficial for enzyme activity. For *OH-2*, K_M was always two to five times lower than for the other enzymes, suggesting that the presence of two hydroxyl groups favors substrate binding. The activities of IMP-1 and *OH-X* are more diverse: with penicillins (PEN and AMP), these two enzymes are equally efficient, whereas *OH-X* is more efficient toward the type I substrates NIT, CEF, and CTX, and IMP-1 is more efficient toward CAZ and IMP. In other words, exchange of the hydroxyl groups of residues 262 and 218 results in altered substrate specificity. Interestingly, the activities of the two enzymes with one hydroxyl group at the two residues were always between those of the enzymes with no and two hydroxyl groups. Adding a hydroxyl group to *OH-0* at position 262 improves conversion of CAZ and IMP, which have positively charged R_2 side-chains, while adding a hydroxyl group at position 218 does not improve CAZ or IMP hydrolysis. Thus, with these substrates the interaction between the hydroxyl group and Lys69 seems to stabilize His263 *via* Pro68 only when the hydroxyl group is at residue 262. Adding a hydroxyl group to either Ala262 or Phe218 improves conversion of PEN and AMP equally, suggesting that with these substrates it is not critical where the hydroxyl group is located. Adding the hydroxyl group at position 262 (IMP-1) does not improve conversion of type I substrates, consistent with the observation that

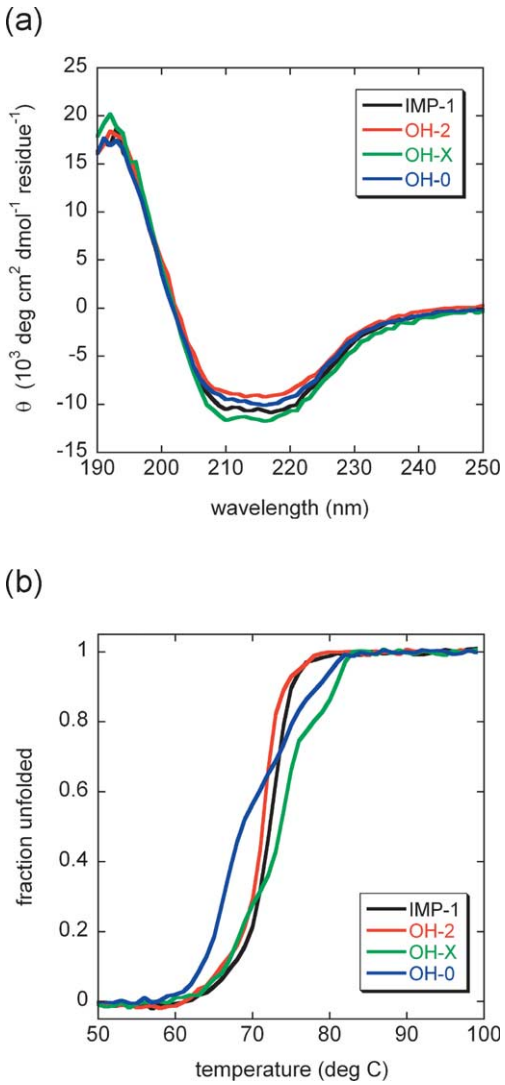

Figure 3. CD experiments with IMP-1 and three mutants in 5 mM sodium phosphate buffer (pH 7.0), containing 100 μM zinc sulfate. (a) For each enzyme, three wavelength scans from 250–190 nm were recorded at 25 °C and averaged. (b) Curves of thermal denaturation. Protein samples were heated from 1 °C to 99 °C in 1 deg. C increments while monitoring CD ellipticity at 218 nm. To facilitate comparison, ellipticities were converted to fraction unfolded.

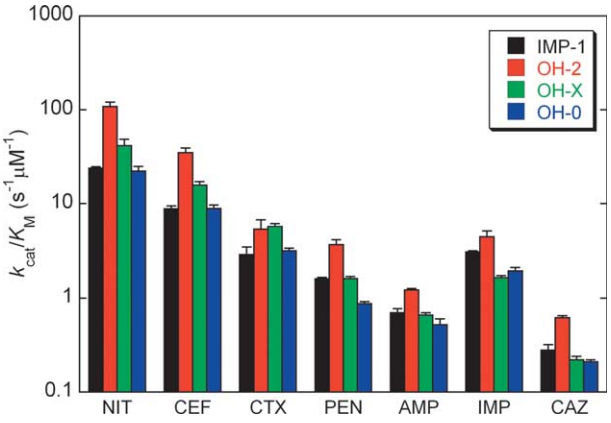

Figure 4. Catalytic efficiency (k_{cat}/K_M) of IMP-1 and three mutants toward seven substrates. Initial velocities were determined and the kinetic constants k_{cat} and K_M were obtained as described.[9] Values are averages of three measurements and the error bars indicate standard deviations. Values for IMP-1 and *OH-0* (IMP-6-G262A) are taken from our earlier work.[9]

the domino effect does not play a role with these substrates.[6,8,9] The reason for the enhanced activity of *OH-X* toward these substrates is not clear and is under further investigation. MD simulations indicate that conformational changes in the Zn2 region of the active site allow for more productive substrate intermediate binding (unpublished results). Interestingly, the beneficial effects of adding a single hydroxyl group to either Ala262 or Phe218 are additive when introducing both groups, resulting in *OH-2* with overall improved catalytic efficiencies. As reported previously,[9] substrate inhibition kinetics[25] was observed for NIT with enzymes that have Tyr at position 218 (*OH-2* and *OH-X*).

The fact that *OH-2* (IMP-1-F218Y) can evolve from IMP-1 by only one nucleotide change and its superior substrate spectrum suggest that this enzyme might be found in clinical isolates in the future. In all published IMP-*n* amino acid sequences, Phe218 is strictly conserved.[26] In codon randomization studies, residue 218 was not mutated because it is remote from the active site.[10,11] Also, an *in vitro* evolution study predicted that IMP-1 cannot evolve to an improved enzyme toward IMP.[27] Indeed, in our hands, the catalytic efficiency of *OH-2* toward IMP was only slightly higher than that of IMP-1 ($4.5(\pm 0.7)\ s^{-1}\ \mu M^{-1}$ compared to $3.1(\pm 0.1)\ s^{-1}\ \mu M^{-1}$). This was not sufficient to confer higher resistance levels to *E. coli* BL21(DE3) host cells expressing *OH-2* compared to cells expressing IMP-1 in minimum inhibitory concentration assays (data not shown). However, it should be kept in mind that IMP-1 is already a very efficient enzyme for a broad spectrum of substrates, and other processes like transport and diffusion of the antibiotic within the cell might limit conversion; this is especially true for our experiments, where the MBL was expressed in the cytoplasm as opposed to the periplasm of the original bacteria.

In conclusion, using computational protein design, we discovered efficient MBL variants that were not found in previous mutagenesis studies and would probably not be expected from bioinformatics approaches due to the strict conservation of Phe218. This underlines the importance and potential of computational

protein design for the investigation and design of enzymes.

Acknowledgements

We thank Jeffrey H. Toney (formerly with Merck) for providing a plasmid containing the IMP-1 gene, Merck for the gift of imipenem, and Marie Ary for assistance with the manuscript. This work was supported by the Howard Hughes Medical Institute, DARPA, the Ralph M. Parsons Foundation, an IBM Shared University Research grant (to S.L.M.) and the Caltech Colvin Fellowship (to P.O.).

Supplementary Data

Supplementary data associated with this article can be found, in the online version, at doi:10.1016/j.jmb.2005.04.044

Details on the kinetic constants can be found in Table S1.

References

1. Carfi, A., Pares, S., Duee, E., Galleni, M., Duez, C., Frere, J. M. & Dideberg, O. (1995). The 3-D structure of a zinc metallo-β-lactamase from *Bacillus cereus* reveals a new type of protein fold. *EMBO J.* **14**, 4914–4921.
2. Garau, G., Garcia-Saez, I., Bebrone, C., Anne, C., Mercuri, P., Galleni, M. *et al*. (2004). Update of the standard numbering scheme for class B β-lactamases. *Antimicrob. Agents Chemother.* **48**, 2347–2349.
3. Fast, W., Wang, Z. G. & Benkovic, S. J. (2001). Familial mutations and zinc stoichiometry determine the rate-limiting step of nitrocefin hydrolysis by metallo-β-lactamase from *Bacteroides fragilis*. *Biochemistry*, **40**, 1640–1650.
4. McManus-Munoz, S. & Crowder, M. W. (1999). Kinetic mechanism of metallo-β-lactamase L1 from *Stenotrophomonas maltophilia*. *Biochemistry*, **38**, 1547–1553.
5. Wang, Z. G., Fast, W. & Benkovic, S. J. (1999). On the mechanism of the metallo-β-lactamase from *Bacteroides fragilis*. *Biochemistry*, **38**, 10013–10023.
6. Iyobe, S., Kusadokoro, H., Ozaki, J., Matsumura, N., Minami, S., Haruta, S. *et al*. (2000). Amino acid substitutions in a variant of IMP-1 metallo-β-lactamase. *Antimicrob. Agents Chemother.* **44**, 2023–2027.
7. Yano, H., Kuga, A., Okamoto, R., Kitasato, H., Kobayashi, T. & Inoue, M. (2001). Plasmid-encoded metallo-β-lactamase (IMP-6) conferring resistance to carbapenems, especially meropenem. *Antimicrob. Agents Chemother.* **45**, 1343–1348.
8. Oelschlaeger, P., Schmid, R. D. & Pleiss, J. (2003). Modeling domino effects in enzymes: molecular basis of the substrate specificity of the bacterial metallo-β-lactamases IMP-1 and IMP-6. *Biochemistry*, **42**, 8945–8956.
9. Oelschlaeger, P., Mayo, S. L. & Pleiss, J. (2005). Impact of remote mutations on metallo-β-lactamase substrate specificity: implications for the evolution of antibiotic resistance. *Protein Sci.* **14**, 765–774.
10. Materon, I. C. & Palzkill, T. (2001). Identification of residues critical for metallo-β-lactamase function by codon randomization and selection. *Protein Sci.* **10**, 2556–2565.
11. Materon, I. C., Beharry, Z., Huang, W., Perez, C. & Palzkill, T. (2004). Analysis of the context dependent sequence requirements of active site residues in the metallo-β-lactamase IMP-1. *J. Mol. Biol.* **344**, 653–663.
12. Concha, N. O., Janson, C. A., Rowling, P., Pearson, S., Cheever, C. A., Clarke, B. P. *et al*. (2000). Crystal structure of the IMP-1 metallo β-lactamase from *Pseudomonas aeruginosa* and its complex with a mercaptocarboxylate inhibitor: binding determinants of a potent, broad-spectrum inhibitor. *Biochemistry*, **39**, 4288–4298.
13. Dunbrack, R. L., Jr & Cohen, F. E. (1997). Bayesian statistical analysis of protein side-chain rotamer preferences. *Protein Sci.* **6**, 1661–1681.
14. Mayo, S. L., Olafson, B. D. & Goddard, W. A. I. (1990). DREIDING: a generic force field for molecular simulations. *J. Phys. Chem.* **94**, 8897–8909.
15. Dahiyat, B. I. & Mayo, S. L. (1997). Probing the role of packing specificity in protein design. *Proc. Natl Acad. Sci. USA*, **94**, 10172–10177.
16. Dahiyat, B. I., Gordon, D. B. & Mayo, S. L. (1997). Automated design of the surface positions of protein helices. *Protein Sci.* **6**, 1333–1337.
17. Street, A. G. & Mayo, S. L. (1998). Pairwise calculation of protein solvent-accessible surface areas. *Fold. Des.* **3**, 253–258.
18. Strop, P. & Mayo, S. L. (1999). Rubredoxin variant folds without iron. *J. Am. Chem. Soc.* **121**, 2341–2345.
19. Desmet, J., Maeyer, M. D., Hazes, B. & Lasters, I. (1992). The dead-end elimination theorem and its use in protein side-chain positioning. *Nature*, **356**, 539–542.
20. Pierce, N. A., Spriet, J. A., Desmet, J. & Mayo, S. L. (2000). Conformational splitting: a more powerful criterion for dead-end elimination. *J. Comput. Chem.* **21**, 999–1009.
21. Huntley, J. J., Fast, W., Benkovic, S. J., Wright, P. E. & Dyson, H. J. (2003). Role of a solvent-exposed tryptophan in the recognition and binding of anti-biotic substrates for a metallo-β-lactamase. *Protein Sci.* **12**, 1368–1375.
22. Moali, C., Anne, C., Lamotte-Brasseur, J., Groslambert, S., Devreese, B., Van Beeumen, J. *et al*. (2003). Analysis of the importance of the metallo-β-lactamase active site loop in substrate binding and catalysis. *Chem. Biol.* **10**, 319–329.
23. Finney, L. A. & O'Halloran, T. V. (2003). Transition metal speciation in the cell: insights from the chemistry of metal ion receptors. *Science*, **300**, 931–936.
24. Periyannan, G., Shaw, P. J., Sigdel, T. & Crowder, M. W. (2004). *In vivo* folding of recombinant metallo-β-lactamase L1 requires the presence of Zn(II). *Protein Sci.* **13**, 2236–2243.
25. Simm, A. M., Higgins, C. S., Pullan, S. T., Avison, M. B., Niumsup, P., Erdozain, O. *et al*. (2001). A novel metallo-β-lactamase, Mbl1b, produced by the environmental bacterium *Caulobacter crescentus*. *FEBS Letters*, **509**, 350–354.
26. Mendes, R. E., Toleman, M. A., Ribeiro, J., Sader, H. S., Jones, R. N. & Walsh, T. R. (2004). Integron carrying a novel metallo-β-lactamase gene, blaIMP-16, and a

fused form of aminoglycoside-resistant gene aac(6′)-30/aac(6′)-Ib′: report from the SENTRY Antimicrobial Surveillance Program. *Antimicrob. Agents Chemother.* **48**, 4693–4702.
27. Hall, B. G. (2004). *In vitro* evolution predicts that the IMP-1 metallo-β-lactamase does not have the potential to evolve increased activity against imipenem. *Antimicrob. Agents Chemother.* **48**, 1032–1033.
28. Koradi, R., Billeter, M. & Wuthrich, K. (1996). MOLMOL: a program for display and analysis of macromolecular structures. *J. Mol. Graph.* **14**, 51–55 see also pp. 29–32.

Edited by J. Thornton

(Received 17 February 2005; accepted 21 April 2005)